

Crystallization and melting in metal-semiconductor multilayers

Walter Sevenhans, Jean-Pierre Locquet, and Yvan Bruynseraede

Laboratorium voor Vaste Stof-Fysika en Magnetisme, Departement Natuurkunde, Katholieke Universiteit Leuven, B-3030 Leuven, Belgium

Hitoshi Homma and Ivan K. Schuller*

Materials Science Division (Building 223), Argonne National Laboratory, Argonne, Illinois 60439-4843

(Received 23 September 1987)

The amorphous-to-microcrystalline phase transition of Ge in Pb/Ge multilayer geometry has been investigated as a function of layer thicknesses with the use of high-temperature x-ray-diffraction techniques. During crystallization, the modulation structure is destroyed and the Pb texture improves. In addition, the crystallization temperature decreases with decreasing amorphous Ge thickness and increases with decreasing thickness of the metallic component. The results imply that the crystallization is interfacially initiated and possibly affected by electron transfer. A study of two-dimensional melting for Pb in this system was attempted unsuccessfully because the layered structure was destroyed by the crystallization that occurs substantially below the melting temperature.

I. INTRODUCTION

Metal-semiconductor multilayers have received considerable attention for a number of years.¹ This has been motivated by the prediction of unusual superconducting phenomena,² the development of novel preparation techniques which allow microscopic control over the thickness of the layers,³ the study of the melting behavior in reduced dimensionality,^{4,5} and their use in important applications such as soft-x-ray mirrors⁶ and electronic devices.⁷ The crystallization of amorphous semiconductors is a problem of considerable interest for the understanding of fundamental kinetic processes as well as in many applications that are subject to thermal cycling. The precise mechanism for the nucleation and growth of a crystalline film starting from an amorphous layer is, however, not well understood. The temperature stability⁸ of metal semiconductor multilayers especially close to the melting temperature has received much less attention. In an interesting experiment,⁵ it was claimed that as the thickness of Pb in Pb/Ge multilayers is reduced, the melting behavior changes from being first order to second order. This is in accordance with theoretical ideas^{4,9} which predict that the melting behavior of a two-dimensional (2D) crystal is of second order. But the nature of the 2D melting is still controversial.

We have undertaken a series of detailed experiments [temperature-dependent x-ray diffraction, transmission electron microscopy (TEM), and electron diffraction] in order to investigate the crystallization of amorphous Ge and the melting behavior of Pb in Pb/Ge multilayers. We find that much below the melting temperature of Pb, the Ge crystallizes, as a consequence of which the Pb texture improves and the layered structure disappears. The crystallization temperature decreases with decreasing Ge thickness (for fixed Pb thickness) and is strongly affected by the texture of the Pb film. This behavior is consistent with the idea that the crystallization is interfacially ini-

tiated and also affected by changes in the Ge electronic structure close to the interface. The melting transition of the Pb film is found to be first order down to the lowest thickness (25 Å) measured. This is probably due to the fact that in these multilayers above the crystallization temperature the layered structure is destroyed, and therefore the material consists of a complicated three-dimensional (3D) Pb network.

II. EARLIER STUDIES

The crystallization of amorphous Ge (*a*-Ge) films has been studied for a number of years in (a) single films ($d > 1000$ Å)¹⁰ for which crystallization temperature is found to be in the range of 350–600 °C; (b) Ge films in contact with a variety of metals (mostly transition and noble)^{11,12} which exhibit a eutectic equilibrium binary-phase diagram, where a correlation was found between the crystallization and eutectic temperatures for a fixed film thickness; and (c) in Ge/Pb multilayers⁵ where it was noticed that the *a*-Ge crystallizes in the temperature range of 135–180 °C; however, no detailed studies were presented.

The dimensional behavior of Pb close to its melting point was also studied in a variety of configurations. It was recently claimed that the melting of the surface of Pb(110) is about 40 °C below the bulk melting temperature.¹³ Small particles of Pb (Ref. 14), on the other hand, exhibit a broad transition although this is probably due to a nonuniform size distribution (i.e., inhomogeneities). The melting of Pb in the Pb/Ge multilayer geometry as measured by differential scanning calorimetry and by the observation of the Pb(111) x-ray-diffraction peak exhibits a broadened transition as the effective Pb layer thickness is reduced.⁵ This was claimed to be due to the transition to 2D in accordance with theories,^{4,9} which predict the melting transition to be of second order in 2D.

III. SAMPLE PREPARATION AND EXPERIMENTAL TECHNIQUES

The reason that Pb/Ge is a particularly favorable system for these types of studies is that in thermodynamic equilibrium Pb and Ge do not form any compounds with a minimum solubility of Pb in Ge and vice-versa,¹⁵ and they have a large difference in melting point (600 °C). Moreover, high-quality multilayers can be prepared with relative ease.

The Pb/Ge multilayers were prepared in a load-locked molecular-beam-epitaxy (MBE) apparatus equipped with two electron-beam guns.¹⁶ The evaporation rates (8 Å/sec for Pb, 5 Å/sec for Ge) were controlled using a quadrupole mass spectrometer in a feedback mode. In this fashion, the evaporation rates could be controlled to better than 5% with a time constant of 3 msec. Pb/Ge multilayers were prepared from 99.999% purity Pb and 99.9999% purity Ge starting materials, using a microprocessor controlled shutter, by alternately exposing the liquid-nitrogen-cooled sapphire substrates to the flux of evaporant. We noticed that small amounts of oxidized Pb changes considerably the temperature-dependent structural behavior, and therefore, we were particularly careful in avoiding oxidation.

X-ray-diffraction measurements were performed in air, Ar atmosphere, and vacuum (10^{-6} Torr with diffusion pump) on a 2 kW DMax II Rigaku diffractometer, equipped with a high-temperature stage (up to 1500 °C) and stabilized better than 1 °C. The crystallinity of the layers was also checked by independent Debye-Scherrer measurements on samples scraped off the substrates. Transverse cross sections for transmission electron microscopy (TEM) and electron diffraction (ED) were prepared using standard thinning techniques including mechanical lapping, dimpling, and ion-beam-sputtering processes. The TEM and ED were performed on a JEOL 100 CX electron microscope equipped with high-temperature capabilities.

IV. RESULTS AND DISCUSSION

A. Initial structure

Small-angle x-ray diffraction from multilayers is a useful tool for the structural characterization of the layered structure. In principle, the small-angle diffraction directly gives the Fourier transform of the composition profile in a multilayer, although quantitative analysis requires dynamic corrections.¹⁷ Therefore, only qualitative conclusions will be drawn from these measurements. Figure 1(a) shows the small-angle diffraction from a [Pb(49 Å)/Ge(59 Å)]₅₀ multilayers, where 50 is the number of bilayers. Up to the eleventh-order low-angle-diffraction peaks can be observed and the even-order peaks have a considerably smaller amplitude than the odd-order ones, as expected. The existence of such a large number of low-angle peaks in conjunction with their intensity variation implies that the layered structure is well developed. We have shown earlier¹⁸ that the thickness variation of the amorphous Ge is continuous and possibly of the order

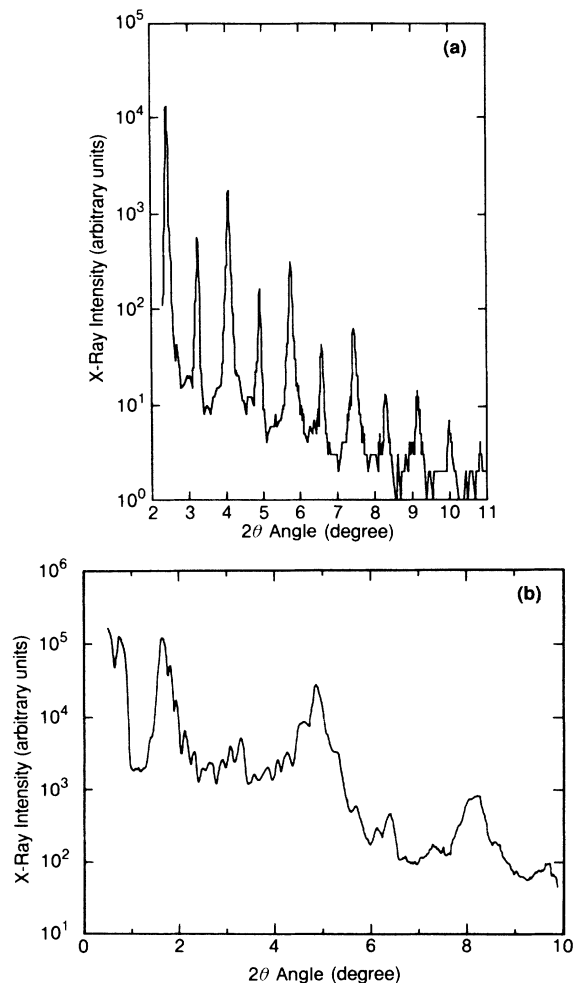


FIG. 1. (a) Small-angle x-ray diffraction from a [Pb(49 Å)/Ge(59 Å)]₅₀ multilayer. The fact that the even-order peaks are smaller in intensity than the odd ones shows that the modulation is square with minimal interdiffusion. (b) Small-angle x-ray diffraction from a [Pb(27 Å)/Ge(27 Å)]₄₈ multilayer. The secondary fringes, next to the Bragg peak, show the high quality of the sample.

of 5% or larger. Figure 1(b) shows the details of the small-angle peaks of a [Pb(27 Å)/Ge(27 Å)]₄₈ sample in an expanded scale. In addition to the Bragg peak, secondary peaks due to the finite number of bilayers are also observable. The existence of these secondary fringes also implies a high quality for the samples since disorder tends to wash out these peaks very fast.

At large angles, the continuous variation of the film thickness in the *a*-Ge broadens the multilayer peaks which in turn limits the perpendicular coherence length to one Pb layer. Consequently, the high-angle diffraction exhibits one Bragg peak corresponding to the Pb(111) texture (broadened by the finite size of the individual Pb layers) in conjunction with the secondary fringes, as shown from the sample of [Pb(50 Å)/Ge(42 Å)]₅₀ in Fig. 2. Note the asymmetry of the large-angle spectrum, i.e., the peak intensities at the low-angle side of the broad peak are higher than those at larger angles. Simple simulations indicate that this is probably due to the expansion of Pb atomic

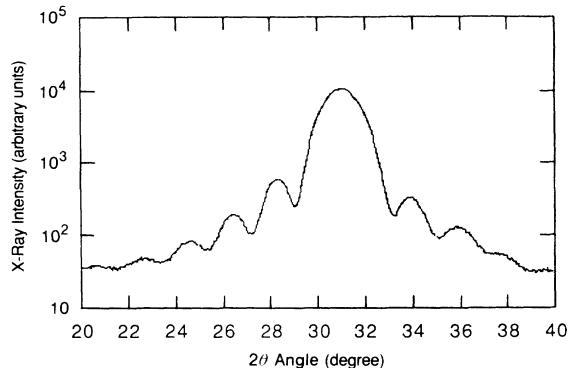


FIG. 2. High-angle x-ray diffraction from a $[\text{Pb}(50 \text{ \AA})/\text{Ge}(42 \text{ \AA})]_{50}$ multilayer. From the typical finite-size-limited diffraction intensity, i.e., one broad peak and secondary maxima, the individual layer thickness of the Pb can be calculated.

layers near the interfaces. The opposite case was reported for the Fe/Ge multilayer system.¹⁹ As the Pb thickness decreases ($d_{\text{Pb}} \leq 40 \text{ \AA}$), a relatively small intensity but very sharp peak comparable to the instrumental resolution starts to appear superposed on top of the finite-size-limited broad peak. This could be explained as due to sample edges, where the Pb layers become connected. From the fact that these samples exhibit well-defined small-angle Bragg peaks, the main portion, with perhaps the exception of the edges, retains the layered structure.

From high-angle ω scans, it was found that the texture of the Pb is quite strongly affected by its thickness. Figure 3 (closed dots) shows that as d_{Pb} increases the Pb(111) texture improves considerably. This is in agreement with expectations which imply a higher degree of order in thicker films for fixed Pb thickness. The rocking curve width, $\Delta\omega$, changes little with d_{Ge} indicating that the amorphous Ge film does not strongly influence the texture of the Pb film (open squares).

B. Crystallization

The crystallization of *a*-Ge (Fig. 4) is accompanied by an improvement on the texture of Pb (Fig. 5) and a loss of the layered structure of the sample as shown in Fig. 6. As

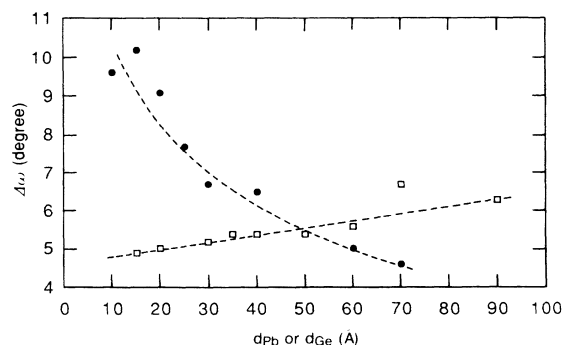


FIG. 3. Rocking curve width $\Delta\omega$ for the Pb(111) peak vs d_{Pb} (●) or d_{Ge} (□).

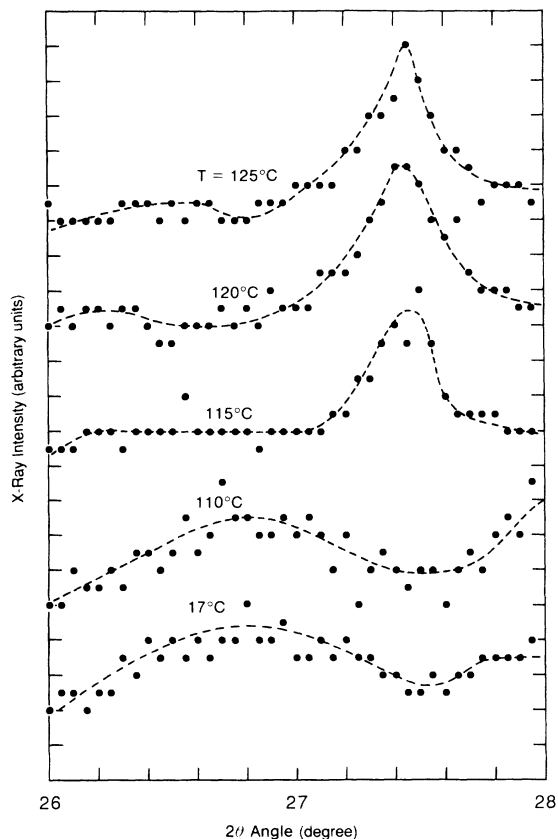


FIG. 4. Temperature evolution of the Ge(111) x-ray peak for a $[\text{Pb}(50 \text{ \AA})/\text{Ge}(42 \text{ \AA})]_{50}$ multilayer.

a function of temperature the increase in the Ge(111) (Fig. 4) peak coincides with an increase of the Pb(111) peak (Fig. 5) and a decrease of the low-angle modulation peaks. We define as the "crystallization temperature" T_x the midpoint of the transition in curves such as shown in Fig. 6. In Fig. 5, the temperature dependence of the Pb(111) peak is plotted. Two important things should be noticed: an increase of the peak intensity and a decrease of the linewidth. The rising intensity, together with the decreasing rocking curve width of the Pb(111) peak (Fig. 7) are clear evidence for an increase in texture. The decrease of the Pb(111) peak linewidth indicates a growing coherency between the Pb(111) planes, because the layers have broken up and separated Pb layers have merged (see also TEM data in Fig. 9). Since the Pb(111) peak is the most intense we characterized the crystallization by studying its dependence as a function of temperature. We have checked that invariably three phenomena [i.e., increase in the Pb(111) and Ge(111) and decrease in the multilayer peak intensities] occur simultaneously. The Ge crystallization may partly cause the improved texture of Pb which in turn releases some heat, along with providing a rough interface.

For the systematic study of the crystallization mechanism, we prepared two series of samples; one keeping $d_{\text{Pb}} = 50 \text{ \AA}$ and another keeping $d_{\text{Ge}} = 50 \text{ \AA}$ constant. Figure 8 shows the crystallization temperature T_x as the function of layer thicknesses (d_{Ge} and d_{Pb}) and rocking

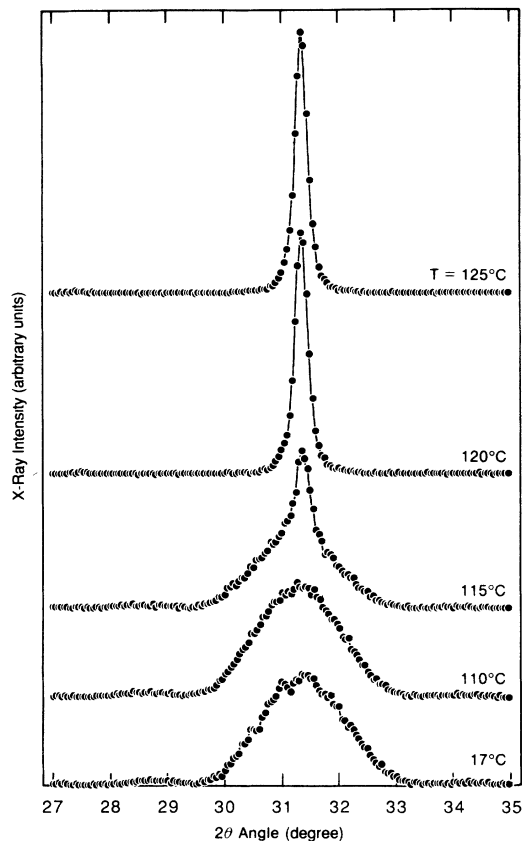


FIG. 5. Temperature evolution of the Pb(111) x-ray peak of a $[\text{Pb}(50 \text{ \AA})/\text{Ge}(42 \text{ \AA})]_{50}$ multilayer.

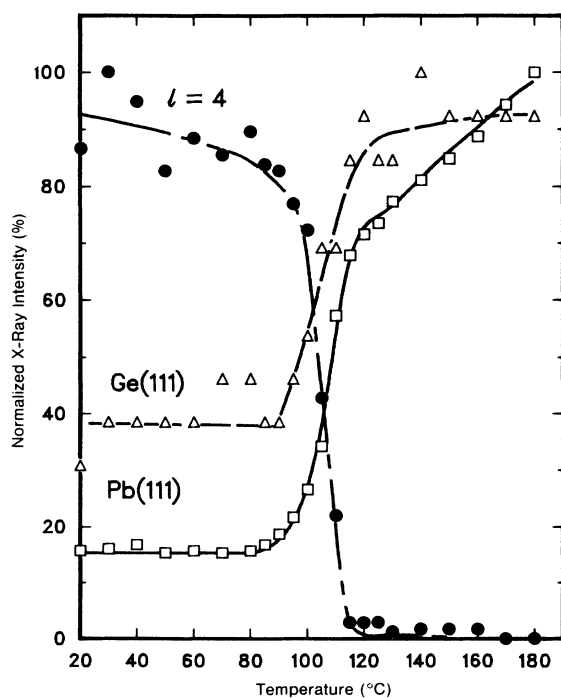


FIG. 6. Temperature dependence of the x-ray intensity for the fourth-order multilayer reflection ($l=4$), the Pb(111), and Ge(111) peaks of a $[\text{Pb}(40 \text{ \AA})/\text{Ge}(50 \text{ \AA})]_{55}$ multilayer.

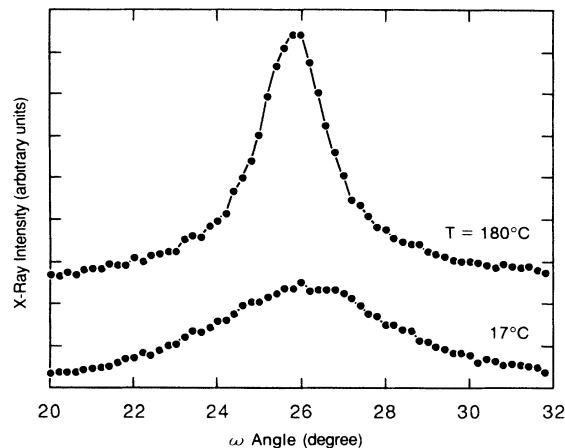


FIG. 7. Rocking curve of the Pb(111) peak in a $[\text{Pb}(50 \text{ \AA})/\text{Ge}(42 \text{ \AA})]_{50}$ at 17°C and 180°C .

curve width ($\Delta\omega$). The dependence of T_x on d_{Ge} , for fixed $d_{\text{Pb}} = 50 \text{ \AA}$ [Fig. 8(a)], shows that as the Ge thickness decreases the crystallization temperature clearly shifts to a lower temperature. On the other hand, Figs. 8(b) and 8(c) show that for a fixed d_{Ge} the crystallization temperature changes if the Pb texture changes. The higher the Pb texture is (i.e., $\Delta\omega$ smaller), the lower the crystallization temperature. We also noticed that the transition width is larger for smaller Ge thicknesses, possibly due to sample inhomogeneities.

Figure 9(a) shows a TEM picture of a cross section of a $[\text{Pb}(120 \text{ \AA})/\text{Ge}(80 \text{ \AA})]_{25}$ multilayer at ambient temperature. Pb and Ge layers correspond to light and dark areas, respectively, in the layered structure. The formation of smooth layers is clearly indicated in the photograph. The electron-diffraction (ED) picture [Fig. 9(b)] shows the existence of crystalline Pb(111) with no evidence of crystalline Ge. After 1 min at $\sim 110^\circ\text{C}$, the layered structure becomes quite rough and is eventually destroyed [Fig. 9(c)]. At the same time, crystalline Ge spots appear in the ED [Fig. 9(d)]. All the electron microscopy measurements thus agree with the x-ray-diffraction experiments.

The present results are also consistent with those of Oki *et al.*¹² however, a detailed comparison cannot be made since Oki *et al.* give very limited information about the layer thickness and preparation conditions.

We have shown earlier that the width of the Pb(111) texture (from rocking curve measurements) changes little for all samples in the $d_{\text{Pb}} = 50 \text{ \AA}$ series (see open squares in Fig. 3). Therefore, for a fixed Pb thickness and a fixed Pb texture, it is easier to crystallize a thinner Ge film (i.e., T_x is lowered) than a thicker one, due to the fact that the crystallization is interfacially initiated.

Based on the above conclusions one might naively expect the crystallization temperature not to change if the d_{Ge} is kept constant. However, this would only occur if the Pb texture remained constant regardless of d_{Pb} , which is not the case (see closed circle in Fig. 3). The fact that a higher Pb texture lowers the crystallization temperature [Fig. 8(c)] is exactly what one might expect if the crystallization is interfacially initiated. Since the Pb acts as a "template" for the Ge, an improved texture of the Pb fa-

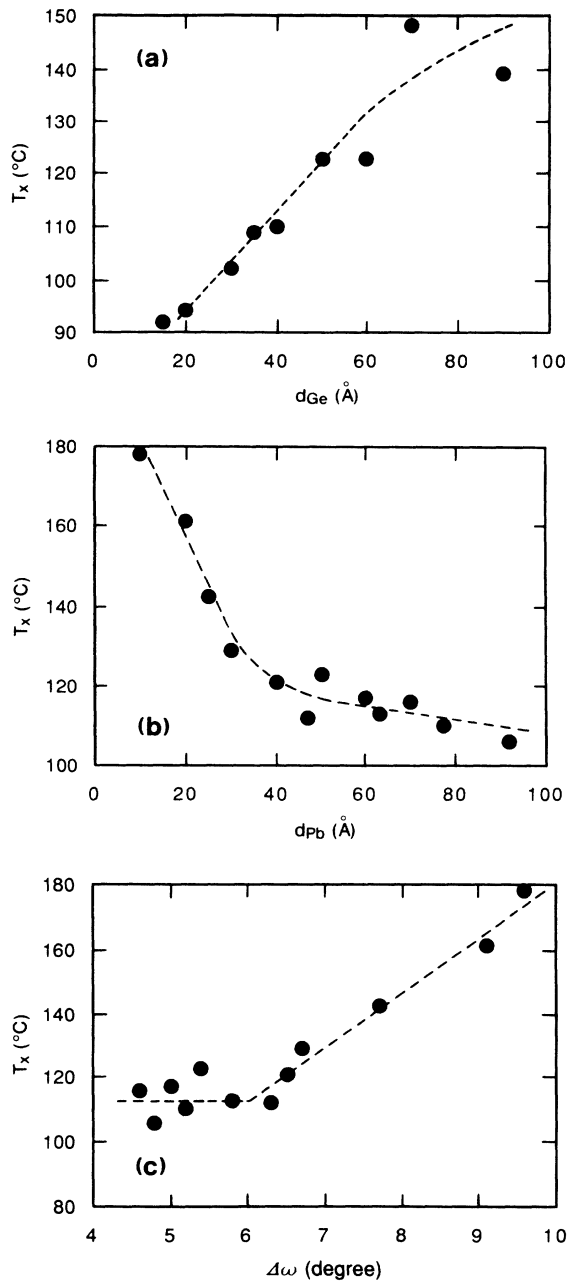


FIG. 8. Crystallization temperature T_x , as a function of (a) d_{Ge} for constant $d_{Pb} = 50$ Å; (b) d_{Pb} , for constant $d_{Ge} = 50$ Å; and (c) Pb(111) rocking curve width ($\Delta\omega$) for constant $d_{Ge} = 50$ Å.

cilitates the Ge crystallization, and therefore lowers the crystallization temperature.

In addition to the “interface-induced” crystallization, changes in the electronic structure also may contribute to the crystallization. When in contact with a metal, the covalent bonding of *a*-Ge or *a*-Si changes into a more metallic one due to electron transfer and this may lower T_x substantially. Auger electron spectroscopy experiments of *a*- and crystalline-Si (*c*-Si), in various environments,^{20,21} show a change of the electronic structure of *a*-Si if in close contact with a noble metal. In the *LVV* spectrum, the typical *c*-Si peak at 92 eV vanishes and is replaced by two

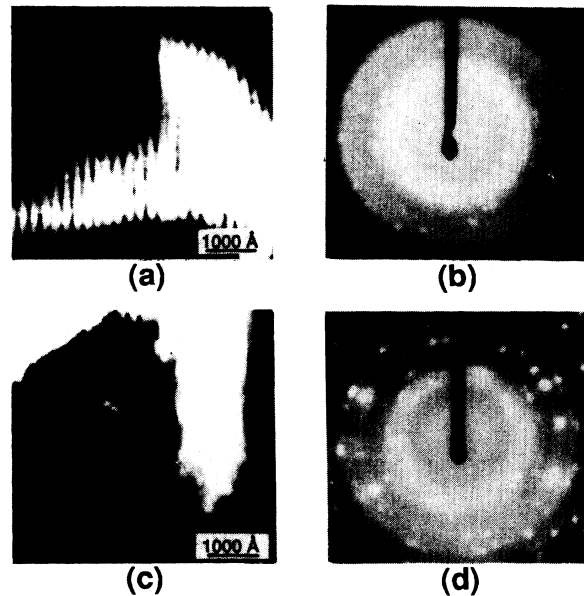


FIG. 9. (a) Transverse cross section (TEM) of a [Pb(120 Å)/Ge(80 Å)]₂₅ multilayer. The layers are clearly observable in these images. (b) ED showing Pb(111) crystalline spots with no trace of crystalline Ge. (c) TEM picture of the sample shown in (a) after annealing. Note that the layered structure is absent. (d) ED of the annealed sample showing crystalline Ge spots.

peaks at 90 and 95 eV, which was interpreted by Hiraki *et al.* as originating from the metallic character of the *a*-Si. This results in weaker bonds between the Si atoms, enhancing the kinetics of the diffusion. Moreover, due to the low mutual solubility of Pb and Ge, Ge will precipitate in the form of crystals, inducing stress in the Pb. This stress is then relieved by an improvement of the Pb texture.

In summary, we have shown that as the Ge crystallizes, the Pb texture improves and the layered structure is destroyed. For fixed d_{Pb} , the crystallization temperature decreases monotonically with d_{Ge} . Moreover, the Pb texture has a dramatic effect on the crystallization temperature. The higher the Pb(111) texture is (i.e., smaller $\Delta\omega$) the lower T_x is. These results show that the Ge crystallization is interfacially initiated that a higher texture of Pb decreases the crystallization temperature and is probably enhanced by the increase of the metallic character of the semiconductor bonds.

C. Melting

In order to study the influence of dimensionality on the melting properties of Pb, Pb/Ge multilayers with varying layer thicknesses were measured up to 340°C in vacuum, air, and Ar atmosphere. A typical temperature dependence of the Pb(111) peak intensity, which characterizes the crystallinity of the Pb, is shown in Fig. 10. The Pb behavior in air is quite different from the results in vacuum or Ar. In air, as the temperature is increased, the transition appeared quite broad ($\sim 10^\circ\text{C}$) and shifted to lower

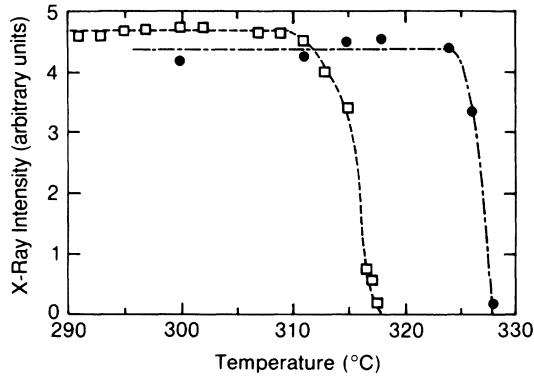


FIG. 10. Pb(111) x-ray peak intensity as a function of temperature for a [Pb(25 Å)/Ge(50 Å)]₆₅ multilayer. Data were taken in air (open squares) and in vacuum (closed circles).

temperatures ($\sim 318^\circ\text{C}$) due to the oxidation of the Pb. The formation of oxides after heating to high temperatures (340°C) in air was confirmed by Debye-Scherrer measurements on samples scraped off the substrate. The measurements in vacuum and Ar showed a sharp transition close to the bulk Pb melting temperature of 327°C . The width of the transition was at most 3°C .

This is not unexpected since as we have shown in Sec. IV B the crystallization of the Ge destroys the layered structure, and therefore, the Pb layers become interconnected in a complicated percolating network. Consequently, the possible 2D character of the Pb film is lost, and therefore transition becomes 3D-like, i.e., sharp with no shift.

V. CONCLUSIONS

The thermal behavior of Pb/Ge multilayers is characterized by a crystallization of the amorphous Ge at temperatures substantially below the sharp melting transition of bulk Pb. As the Ge crystallizes, the Pb(111) texture improves and the layered structure is lost. This behavior implies that the crystallization is interfacially initiated, that the higher the texture of Pb the lower the crystallization temperature, and is possibly affected by electron transfer from Pb into the Ge. Perhaps these findings regarding crystallization are of a more general nature, apply to other systems, and therefore should be further tested experimentally.

As far as melting is concerned our measurements imply that the Pb/Ge multilayered system is not suitable for studying the problems of 2D melting.⁵

ACKNOWLEDGMENTS

We would like to thank Y. L epetre, H. Ho, R. Kampwirth, E. Ziegler, F. Spaepen, R. Willens, and M. Van Rossum for helpful discussions. This work was supported by the U.S. Office of Naval Research Contract No. N00014-83-F-0031 and the U.S. Department of Energy (Division of Materials Sciences, Office of Basic Energy Sciences) under Contract No. W-31-109-ENG-38 at Argonne National Laboratory and Contract No. DE-FG03-87ER45332 at University of California-San Diego. International travel was provided by North Atlantic Treaty Organization (NATO) Grant No. RG85/0695 and the Belgian National Science Foundation.

*Present address: Physics Department B019, University of California-San Diego, La Jolla, CA 92093.

¹See, for instance, M. Strongin, O. F. Kammerer, J. E. Crow, R. D. Parks, D. H. Douglass, Jr., and M. A. Jensen, *Phys. Rev. Lett.* **21**, 1320 (1968).

²D. Allender, J. Bray, and J. Bardeen, *Phys. Rev. B* **7**, 1020 (1973).

³For a recent review, see *Synthetic Modulated Structures*, edited by L. L. Chang and B. C. Giessen (Academic, New York, 1985).

⁴J. M. Kosterlitz and D. J. Thouless, *J. Phys. C* **6**, 1181 (1973).

⁵R. H. Willens, A. Kornblit, L. R. Testardi, and S. Nakahara, *Phys. Rev. B* **25**, 290 (1982); G. Devoud and R. H. Willens, *Phys. Rev. Lett.* **57**, 2683 (1986).

⁶See, for instance, E. Spiller, A. Segm uller, J. Rife, and R. P. Haelbich, *Appl. Phys. Lett.* **37**, 1048 (1980); J. H. Underwood and T. W. Barbee, *Nature* **194**, 492 (1981).

⁷See, e.g., *Conference Record of Seventeenth IEEE Photovoltaic Specialists Conference* (IEEE, New York, 1984).

⁸E. Ziegler, Y. L epetre, I. K. Schuller, and E. Spiller, *Appl. Phys. Lett.* **48**, 1354 (1986).

⁹B. I. Halperin and D. R. Nelson, *Phys. Rev. Lett.* **41**, 121 (1973).

¹⁰A. Barna, P. B. Barna, and J. F. Poczka, *J. Non-Cryst. Solids* **10**, 361 (1972).

¹¹E. Oki, Y. Ogawa, and Y. Fujiki, *J. Appl. Phys.* **8**, 1056 (1969).

¹²T. D. Moustakas, in *Tetrahedrally-Bonded Amorphous Semiconductors*, edited by D. Adler and H. Fritzsche (Plenum, New York, 1985), p. 93.

¹³J. W. M. Frenken and J. F. van der Veen, *Phys. Rev. Lett.* **54**, 134 (1985); J. W. M. Frenken, P. M. J. Maree, and J. F. van der Veen, *Phys. Rev. B* **34**, 7506 (1986).

¹⁴R. Garrigos, R. Kofman, P. Cheyssac, and M. Y. Perrin, *Europhys. Lett.* **1**, 355 (1986).

¹⁵M. Hansen, *Constitution of Binary Alloys* (McGraw-Hill, New York, 1958), and supplements.

¹⁶W. Sevenhans, J. P. Locquet, and Y. Bruynseraede, *Rev. Sci. Instrum.* **57**, 937 (1986).

¹⁷A. Guinier, *X-Ray Diffraction in Imperfect Crystals, and Amorphous Bodies* (Freeman, San Francisco, 1963), p. 111.

¹⁸W. Sevenhans, M. Gijs, Y. Bruynseraede, H. Homma, and I. K. Schuller, *Phys. Rev. B* **34**, 5955 (1986).

¹⁹C. F. Majkrzak, J. D. Axe, and P. B oni, *J. Appl. Phys.* **57**, 3657 (1985).

²⁰A. Hiraki, A. Shimizu, M. Iwami, T. Narusawa, and S. Komiyama, *Appl. Phys. Lett.* **26**, 57 (1975).

²¹K. Nakashima, M. Iwami, and A. Hiraki, *Thin Solid Films* **21**, 423 (1975).

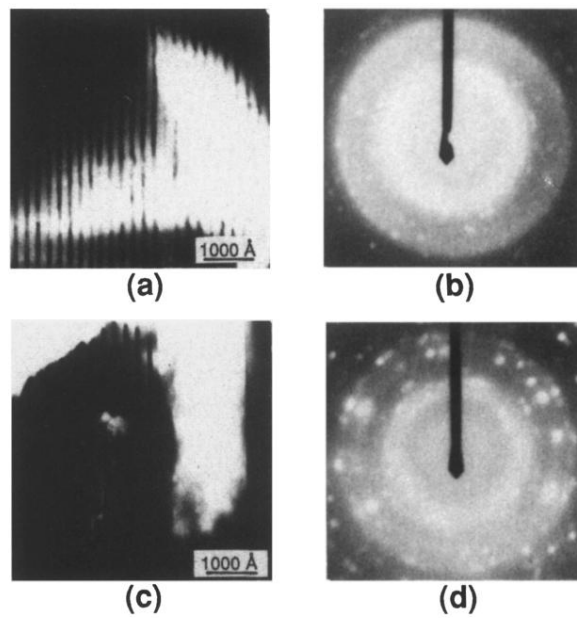


FIG. 9. (a) Transverse cross section (TEM) of a [Pb(120 Å)/Ge(80 Å)]₂₅ multilayer. The layers are clearly observable in these images. (b) ED showing Pb(111) crystalline spots with no trace of crystalline Ge. (c) TEM picture of the sample shown in (a) after annealing. Note that the layered structure is absent. (d) ED of the annealed sample showing crystalline Ge spots.